Energy Proceedings
Vol 54, 2025
ISSN 2004-2965

Optimization of the pulverized system of the coal-fired power plant by revising control strategy#

Liqun Xie, Chaoyang Wang*, Zefeng Liu, Ming Liu, Junjie Yan

State Key Laboratory of Multiphase Flow in Power Engineering, Xi'an Jiaotong University, Xi'an, 710049, China

(Email: chaoyang.wang@xjtu.edu.cn)

ABSTRACT

During load cycling processes of coal-fired power plants, the MPS pulverizers system's response time dominates the power unit's operation flexibility. Reducing the effect of the delay and inertia of the pulverizing system is urgent. This study established and validated a complete pulverizing system model, which included six coal mills, coupling with an established coal-fired power plant model. A revised fuel demands control strategy based on the main-auxiliary coordination was proposed. The results show that by implementing the revised control strategy, the absolute pulverized coal output deviation was reduced by up to 216 kg, 126kg, and 116kg, respectively, with three operating modes. When four coal mills were operational, the reduction constituted 0.09% of the pulverizing system's output during the load transition. The new control strategy enhanced the matching of the main and auxiliary systems in coal-fired power units.

Keywords: energy efficiency, power plant, pulverizing system, control scheme optimization

1. INTRODUCTION

Energy is the principal arena for reducing carbon emissions and is vital to the solutions. An advanced power system is being rapidly developed in China. The proportion of coal-fired power capacity in China's energy mix fell below 40% for the first time, while the installed capacity of non-fossil-based power generation surpassed 1000 GW by the end of 2023 [1]. However, the volatility and intermittency of renewable energy sources pose significant challenges to grid stability. It is imperative to enhance operational flexibility and efficiency for coal-fired power plants. The research on configuration reformation [2] and coupling with external devices [3-4] have gained widespread attention, while in-depth studies on internal components, particularly the energy source — the pulverizing system—remain insufficient. With the increasing demand for load-following and frequency regulation in coal-fired power units, the constraints and optimization potential of the pulverizing system on unit flexibility and efficiency should be thoroughly investigated.

The pulverizing system encounters challenges such as significant inertia, strong coupling, and delayed response during load cycling processes [5]. To enhance the output responsiveness of the pulverizing system, it is crucial to develop an accurate model. Gao et al. [6] proposed a coal mill model that considers the effect of coal moisture on its accuracy, and the model can effectively represent the mid-high process of coal mill dynamics and estimate the key parameters in coal mills. Łabęda-Grudziak et al. [7] monitored the temperature of a dust–air mixture at the outlet of a coal mill using an additive regression model and data mining techniques, thereby improving the usability of the statistical modeling. Hu et al. [8] established a dynamic coal mill model with sufficient accuracy and adaptability, which can be used for fault simulation. The mill pulverizing system is a complex nonlinear system having a strong coupling among the variables. Pulverized fuel flow and other internal states of the mill are unmeasurable [9]. Establishing effective control strategies is particularly crucial. Wang et al. [10] proposed a power-saving control strategy for the primary air fan, which decreased the fans' power consumption while maintaining the mill outlet temperature within the optimum range. Liang et al. [11] developed an inferential multi-mode predictive control scheme based on moving horizon estimation for the pulverizing system. Gao et al. [12] designed an optimized output control scheme for the pulverizing system on the basis of the estimation of the outlet coal powder flow of the mill, which improved the tracking ability and control precision of the pulverizing system's output. Overall, the majority of studies focused on modeling and control algorithms for individual coal mills. However, there is still a lack of research on mechanistic models and control strategies for the complete pulverizing system, especially when coupled with coal-

This is a paper for the 16th International Conference on Applied Energy (ICAE2024), Sep. 1-5, 2024, Niigata, Japan.

fired power plants, considering the energy efficiency across a wide range of load changes.

This study aims to tackle these gaps by providing a comprehensive pulverizing system model consisting of six MPS coal mills integrated into the thermal system. The dynamic performance of the pulverizing system during the load cycling process was simulated and analyzed. An optimized fuel control strategy considering the main-auxiliary coordination was proposed to enhance the pulverizing system's responsiveness.

2. MODELINGS

Our previous work has presented detailed modeling procedures for the coal-fired power plant [13]. Fig. 1 illustrates the schematic of a 660 MW ultra-supercritical coal-fired power plant integrated with an MPS medium-speed mill direct-fired pulverizing system, consisting of six MPS190HP-II type coal mills. This study has developed a comprehensive dynamic simulation model of the MPS pulverizer, which is the foundation of transient operation optimization of the pulverizing system.

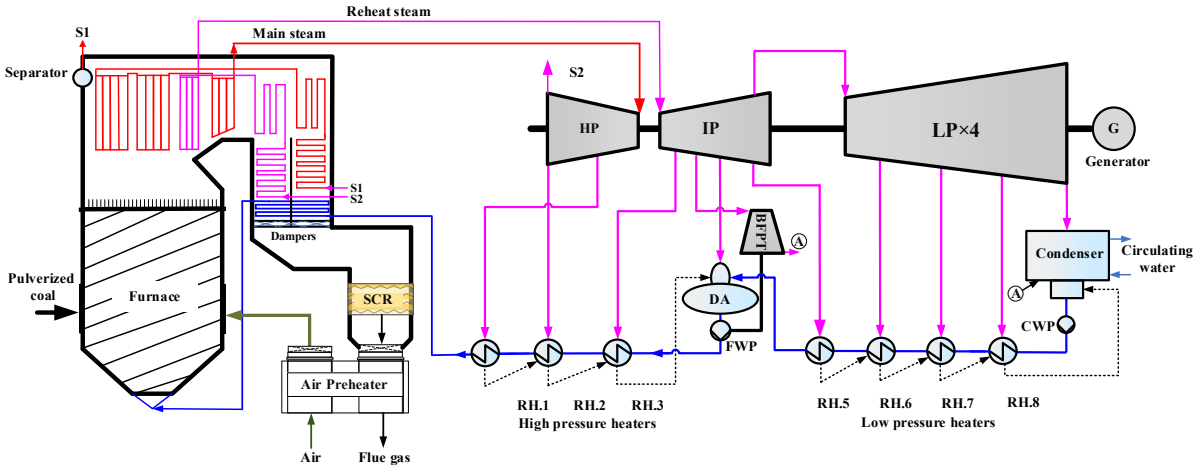

Fig. 1. Schematic diagram of 660 MW ultra-supercritical power unit

2.1 Dynamic model of the MPS pulverizer

The model was constructed using an MPS190 HP-II coal mill. The mill's operation involves the motor-driven rotation of a grinding table, with rollers rotating in tandem. Raw coal is delivered via a feeder, descending onto the table. Centrifugal force propels the coal through a grinding zone created by the interaction between the rollers and the table. The combined forces of the rollers' weight and the downward pressure from the loading device crush the coal, which is further pulverized by the friction generated from the relative motion between the rollers and the table. Primary air, introduced through the air port ring, fluidizes and transports the pulverized coal towards the classifier, facilitating heat exchange. Within the classifier, the coal-air mixture is directed through angled openings, inducing a spin that generates centrifugal force. Coarser particles are separated by impacting the perimeter and falling back into the grinding zone, while finer particles remain suspended in the air mixture and are directed to the fuel conduits, then supplied to the furnace for combustion.

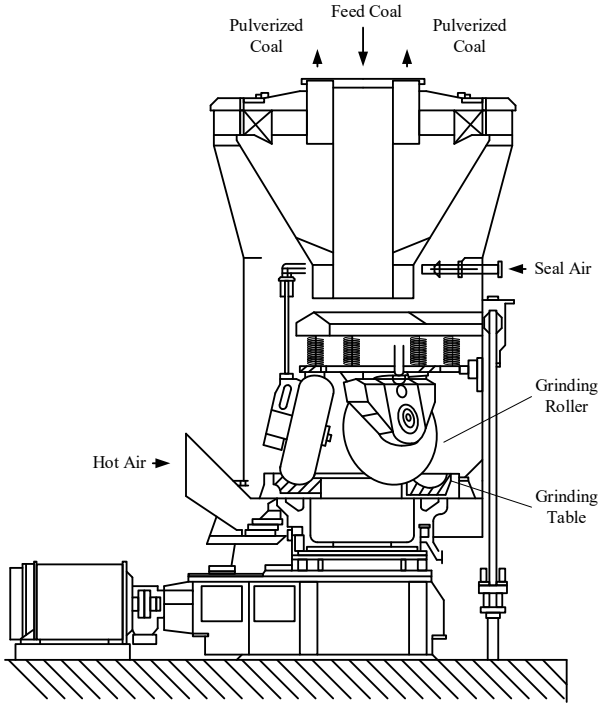

Fig. 2. The structure of the MPS mill

Fig. 2 depicts the structural configuration of the mill. The model partitions the MPS mill into the table and grinding zones. The table zone includes the entire upper

surface of the mill untouched by the rollers, while the grinding zone encompasses the interface between the grinding table and the rollers. The model integrates mass conservation and heat balance equations for each zone. Additionally, equations for mill differential pressure and mill current are formulated within the model.

2.1.1 The table zone of the mill

Based on mass balance, the equation for coal on the grinding table can be formulated as Eq. (1):

$$\frac{\mathrm{d}M_{\mathrm{raw}}}{\mathrm{d}\tau}=B_{\mathrm{feed}}+B_{\mathrm{back}}-B_{\mathrm{raw}} \tag{1}$$

Where M_{raw} is the mass of raw coal on the grinding table, kg; B_{feed} is the mass flow rate of coal feed, kg s^{-1}; B_{back} is the mass flow rate of coal returning to the table, kg s^{-1}; B_{raw} is the mass flow rate of coal from table zone to the grinding zone, kg s^{-1}.

The movement of coal relative to the grinding table is characterized by uniformly variable linear motion. The mass flow rate of coal from the table zone to the grinding zone can be determined as follows:

$$B_{\mathrm{raw}}=\frac{M_{\mathrm{raw}}}{t} \tag{2}$$

where t is the time required for raw coal to enter the grinding zone from the center of the table, s;

The energy balance equation of the table zone can be formulated as Eq. (3):

$$Q_{\mathrm{in,table}}-Q_{\mathrm{out,table}}=\left[c_{\mathrm{raw}}\left(1-m_{\mathrm{ar}}\right)+c_{\mathrm{water}}m_{\mathrm{ar}}\right]M_{\mathrm{raw}}\frac{dt_{\mathrm{raw}}}{d\tau} \tag{3}$$

Where $Q_{in,table}$ is the heat input per unit time, kW; $Q_{out,table}$ is the heat output per unit time, kW; c_{raw} and c_{water} are the specific heat capacities of raw coal and water, kJ kg^{-1} ℃$^{-1}$; m_{ar} is the moisture content of raw coal, %; t_{raw} is the temperature of the raw coal, ℃.

2.1.2 The grinding zone of the mill

On the basis of mass balance, the equations for coal in the grinding zone can be established as follows:

$$\frac{\mathrm{d}M_{\mathrm{c}}}{\mathrm{d}\tau}=B_{\mathrm{raw}}-B_{\mathrm{sz}}-k_{\mathrm{c}}M_{\mathrm{c}} \tag{4}$$

$$\frac{\mathrm{d}M_{\mathrm{pf}}}{\mathrm{d}\tau}=k_{\mathrm{c}}M_{\mathrm{c}}-B_{\mathrm{left}} \tag{5}$$

Where M_c is the mass of raw coal in the grinding zone, kg; M_{pf} is the mass of pulverized coal in the grinding zone, kg; B_{sz} is the mass flow of pulverized rejects, kg s^{-1}; k_c is the conversion coefficient of raw coal to pulverized coal, %; Both raw coal and pulverized coal coexist in the grinding zone. The mass flow rate of the coal exiting the grinding zone is proportional to the mill's primary air velocity and the mass of pulverized coal in the grinding zone. Consequently, the mass flow rate of coal leaving the grinding zone can be computed as:

$$B_{\mathrm{left}}=\frac{k_2q_{\mathrm{air,out}}M_{\mathrm{pf}}}{\rho_{\mathrm{air,out}}} \tag{6}$$

Where B_{left} is the mass flow of the coal exiting the grinding zone, kg s^{-1}; $q_{air,out}$ is the mass flow of primary air, kg s^{-1}; $\rho_{air,out}$ is the density of primary air, kg m^{-3}; k_2 is an identified parameter.

After leaving the grinding zone, the pulverized coal is entrained into the classifier. Therefore, B_m can be represented as follows:

$$B_{\mathrm{back}}=B_{\mathrm{left}}-B_{\mathrm{m}} \tag{7}$$

$$B_{\mathrm{m}}=\frac{k_3q_{\mathrm{air,out}}T_{\mathrm{m}}}{\rho_{\mathrm{m}}} \tag{8}$$

Where B_m is the mass flow of outlet pulverized coal, kg s^{-1}; T_m is the temperature of the coal-air mixture, K; ρ_m is the density of the pulverized coal, kg m^{-3}; k_3 is an identified parameter.

The energy balance equation for the grinding zone can be formulated as Eq. (9):

$$Q_{\mathrm{in,grinding}}-Q_{\mathrm{out,grinding}}=\left\{\left[c_{\mathrm{pf}}\left(1-m_{\mathrm{pf}}\right)+c_{\mathrm{water}}m_{\mathrm{pf}}\right]\left(M_{\mathrm{c}}+M_{\mathrm{pf}}\right)+c_{\mathrm{metal}}m_{\mathrm{metal}}\right\}\frac{dt_{\mathrm{m}}}{d\tau} \tag{9}$$

Where $Q_{in,grinding}$ is the heat input per unit time for the grinding zone; $Q_{out,grinding}$ is the heat output per unit time of the grinding zone; c_{pf} and c_{metal} are the specific heat capacities of pulverized coal and metal steel, kJ kg^{-1} ℃$^{-1}$; m_{metal} is the mass of metal involved in the heat exchange, kg; t_m is the temperature of the coal-air mixture, ℃.

2.1.3 Equation of mill electricity and mill differential pressure

The current I_c is related to the no-load current, B_{feed}, M_c, M_{pf}, and the loading pressure from the pressurizing device. I_c can be computed as:

$$I_{\mathrm{c}}=i_1+i_2B_{\mathrm{feed}}+i_3B_{\mathrm{feed}}^2+i_4B_{\mathrm{feed}}^3+c_1M_{\mathrm{c}}+c_2M_{\mathrm{pf}}+c_3P_{\mathrm{f}} \tag{10}$$

Where I_c is the mill electricity current, A; P_f is the loading pressure from the pressurizing device, MPa; i_1, i_2, i_3, i_4, c_1, c_2, and c_3 are the parameters to be identified.

The pressure loss ΔP of the primary air passing through the mill, accounting for the pressure loss of airflow in the pipeline, coal-air mixture, and the return coal, can be established as:

$$\Delta P=p_1\frac{q_{\mathrm{air,in}}^{\ 2}}{2\rho_{\mathrm{air,in}}}+\left(p_2+p_3\frac{B_{\mathrm{m}}+B_{\mathrm{back}}}{q_{\mathrm{air,in}}}\right)\frac{q_{\mathrm{air,out}}^{\ 2}}{2\rho_{\mathrm{air,out}}}+p_4B_{\mathrm{back}} \tag{11}$$

Where ΔP is the differential pressure, kPa; $\rho_{air,in}$ and $\rho_{air,out}$ are the densities of the inlet and outlet air, kg m^{-3}; p_1, p_2, p_3, and p_4 are the parameters to be identified.

2.2 Control strategy of the pulverizing system

The pulverizing system's control strategy primarily governs the mass flow of primary air and the pulverizer's outlet temperature, as depicted in Fig. 3. The coal-air mixture velocity in the fuel conduits must be carefully regulated to ensure the efficient transport of pulverized coal to the furnace. The hot air damper controls the mass flow of primary air using a feedforward-feedback mechanism, which enhances response speed to variations in coal feed rate and corrects deviations via feedback. The outlet temperature regulator also influences the feedforward signal for the hot air damper, ensuring the primary air mass flow remains optimal while stabilizing the outlet temperature.

To ensure the safe and efficient operation of the boiler, the coal-air mixture temperature at the pulverizer outlet must be maintained within an acceptable range. The temperature controller's setpoint is manually determined based on engineering experience. Control commands for the cold and hot air dampers function as cross feedforward signals, enhancing the system's responsiveness.

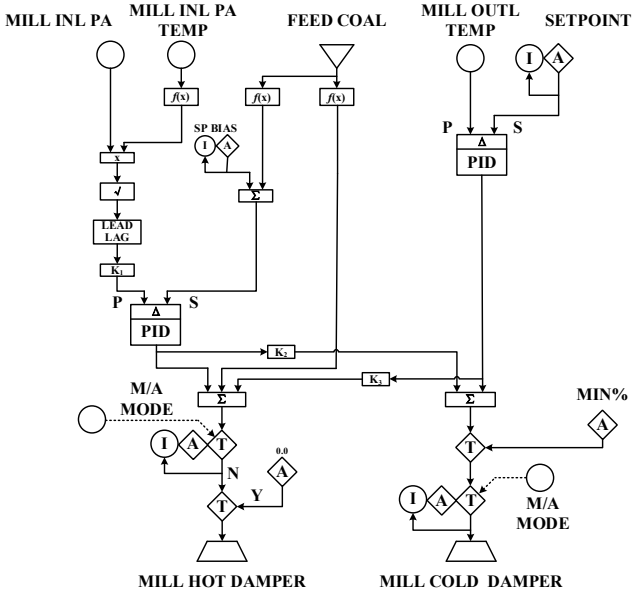

Fig. 3. Control schemes for the hot and coal damper

2.3 Model validation

Our former work has validated and studied the thermal system model [14]. This study utilized historical dates of normal operation to validate the pulverizing system model. Fig. 4 illustrates the temporal variation in boundary conditions, including the mass flow rate of feed coal, mass flow, and temperature of inlet primary air.

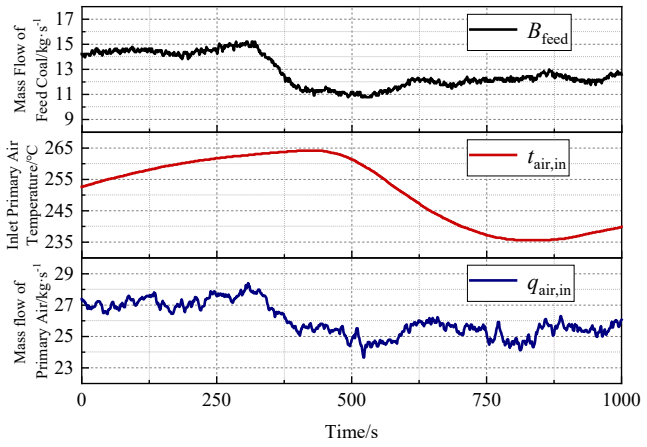

Fig. 4. Boundary condition of MPS mill for the model validation

Fig. 5 presents a comparison of key parameters. As shown, a decrease in the coal feed rate caused the mill's drying capacity to exceed the demand, slightly raising the outlet temperature. The differential pressure and electric current were positively correlated with the coal feed rate, with the simulated values decreasing accordingly, further confirming the model's reliability. Moreover, the simulated values closely matched the measured values in terms of trend, with deviations remaining within the specified range, underscoring the model's high accuracy.

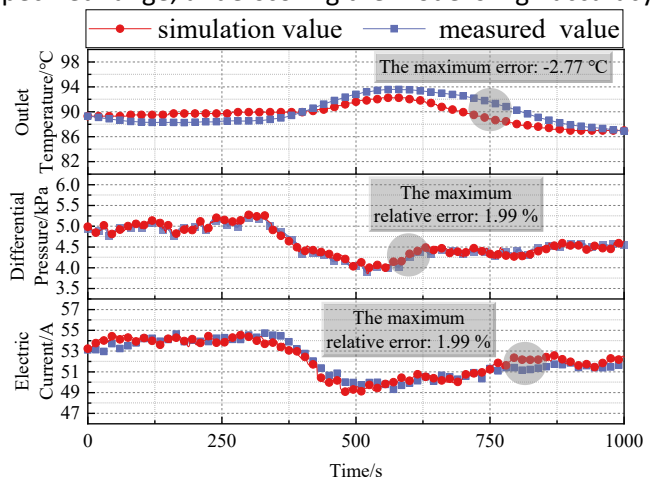

Fig. 5. Curve of the key parameters for model validation

3. METHODOLOGY

3.1 Optimize fuel supply by main-auxiliary coordination.

The pulverizing system is among the most crucial auxiliary systems, with the pulverizer serving as the central component. Due to the challenges associated with engineering measurements, directly determining the real-time mass flow rate of pulverized coal is currently not feasible. Additionally, the inertia and delay inherent in the pulverizing system complicate the accurate measurement of the total coal feed from each

feeder. Consequently, devising an effective control strategy for the pulverized coal output has been challenging. This study developed a reliable MPS medium-speed pulverizer direct-firing system model, integrating key equipment parameters, including pulverized coal output. Leveraging precise real-time output calculations, control strategies were devised for each pulverizer to improve system responsiveness.

Thermal power plants exhibit significant thermal inertia due to heat storage in the boiler metal and the regenerative heating system. Our previous research [14] showed that minimizing the deviation between real-time and steady-state heat storage in the system improves load response and energy efficiency in supercritical coal-fired units. This study seeks to enhance the unit's rapid load-changing capability by adjusting fuel demand setpoints, refining control strategies, and eliminating real-time deviations in heat storage within the main engine. By considering both the main and auxiliary engines, this study aims to optimize the fuel control strategy to enhance peak shaving capabilities and achieve coordinated operation within the unit's main and auxiliary engines.

3.2 Optimization of the control strategy

Fig. 3 illustrates the original control scheme of the pulverizing system, where air temperature and volume are regulated solely by adjusting the hot and cold air dampers. In contrast, Fig. 6 introduces an output control strategy that uses the deviation between real-time output and the setpoint of a single coal mill as input for the PID regulator. The pulverized coal output setpoint is determined by load demand, and this output value is incorporated into the fuel demand to minimize output deviations. For simplicity, a single mill in the diagram represents the output control scheme for all six coal mills.

Real-time heat storage can be calculated from temperature and pressure, with detailed procedures provided in our previous work [15]. The corresponding steady-state heat storage is determined from the real-time load. The deviation in heat storage is adjusted using a conversion factor, which translates this deviation into a modification of the feedforward value for fuel demand, thereby promptly compensating for any thermal storage deficit during the load cycling process.

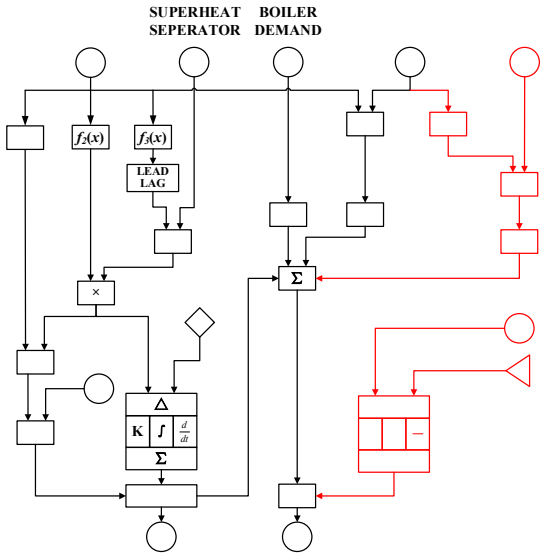

Fig. 6. Revised control scheme for the fuel supply

An optimized fuel command signal has been derived, addressing both the main and auxiliary engines. The two strategies will be introduced in different sequences to evaluate the effectiveness of the two strategies further and achieve optimal results. The output control strategy will be introduced as Scheme I. Building upon this, the thermal storage correction term will be added as Scheme II.

3.3 Energy efficiency characteristics for transient performances

The absolute output deviation (ΔB) reflects the degree of discrepancy between the coal feed rate and the pulverized coal output during load ramping-up processes and serves as a representative parameter for evaluating the response of the pulverizing system. ΔB is defined as follows:

$$\Delta B = \int_0^{\tau_0} \left| B_{\mathrm{gm}} - B_{\mathrm{m}} \right| d\tau \tag{12}$$

4. RESULTS AND DISCUSSIONS

4.1 Real-time pulverized coal output response analysis of the revised control strategy during load ramping-up transient processes.

The pulverizing system comprises six MPS190HP-II coal mills, with four mills operating at 75% THA and five at 100% THA under stable conditions. This study examined three operational modes: maintaining four mills, maintaining five mills, and transitioning from four to five mills. Feed and pulverized coal mass flow rates are critical indicators for coal-fired power plants during transient processes. As illustrated in Fig. 7, these modes' real-time coal mass flow rates were analyzed during load

cycling, with V_e=1.5% Pe min^{-1} as an example. Fig. 7(a) shows that when four mills (A, B, C, and D) were operational, they received equal raw coal feed and operated under identical conditions. In Fig. 7(b), with five mills (A, B, C, D, and E) running, each mill operated at a lower load than in the four-mill configuration. It was transitioning from four to five mills involved in starting up Mill E, as depicted in Fig. 7(c). During the load ramp-up process, Mills A, B, C, and D initially increased their raw coal feed to the target value and stabilized. Mill E was subsequently started, gradually increasing its coal feed and contributing to the overall load. Once Mill E's load equaled that of the other four mills, the pulverizing system's load was evenly distributed across all five mills.

At 75% THA steady-state conditions, the rated total coal consumption is 47.51 kg s^{-1}, while at 100% THA, it increases to 61.52 kg s^{-1}. As shown in Fig. 7, during the load ramp-up process, real-time coal consumption temporarily exceeded the target operating condition (black dashed line). This excess, termed "additional coal consumption" in previous work, diminished to nearly zero as the transient processes concluded. Regardless of the operational mode, the optimized control strategy ensured that pulverized coal output closely matched the corresponding steady-state coal consumption, resulting in more stable coal flow and reduced fluctuations.

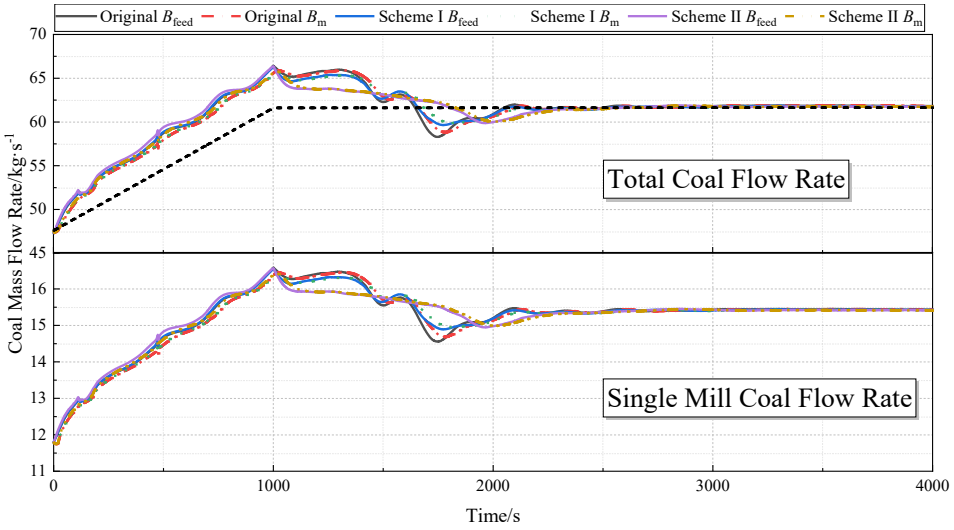

(a)

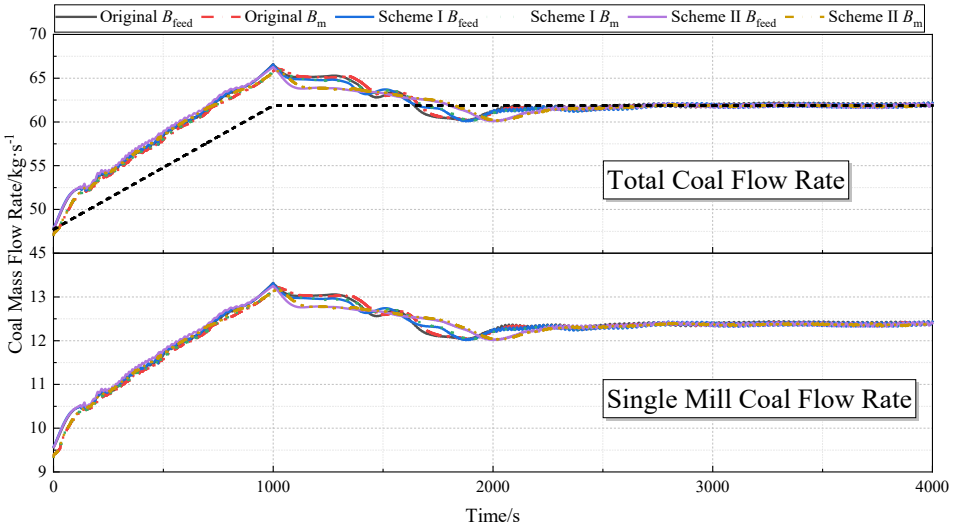

(b)

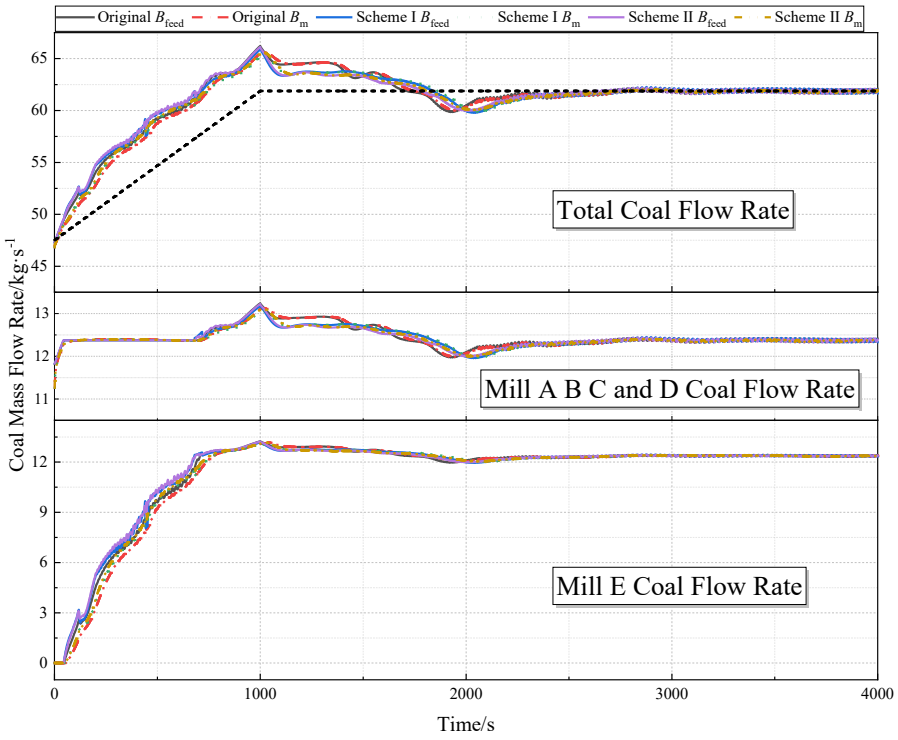

(c)

Fig. 7. Real-time coal consumption during transient processes with V_e=1.5% Pe min^{-1}. (a) four mills in operation; (b) five mills in operation; and (c) four to five mills in operation.

Fig. 8 illustrates the real-time pulverized coal output under three different operating modes when V_e equals 2.0% Pe min^{-1}, reflecting the performance of the pulverizing system and each coal mill. During the load ramp-up phase, as the load change rate increased, the original control strategy sharply increased coal feed demand, causing the coal feed curve to steepen. This caused a greater deviation between the real-time output and the coal feed corresponding to the steady state. However, with the optimized control strategy, the coal feed curve closely approximates the steady-state model, significantly reducing fluctuations in coal feed and achieving the final steady state more rapidly.

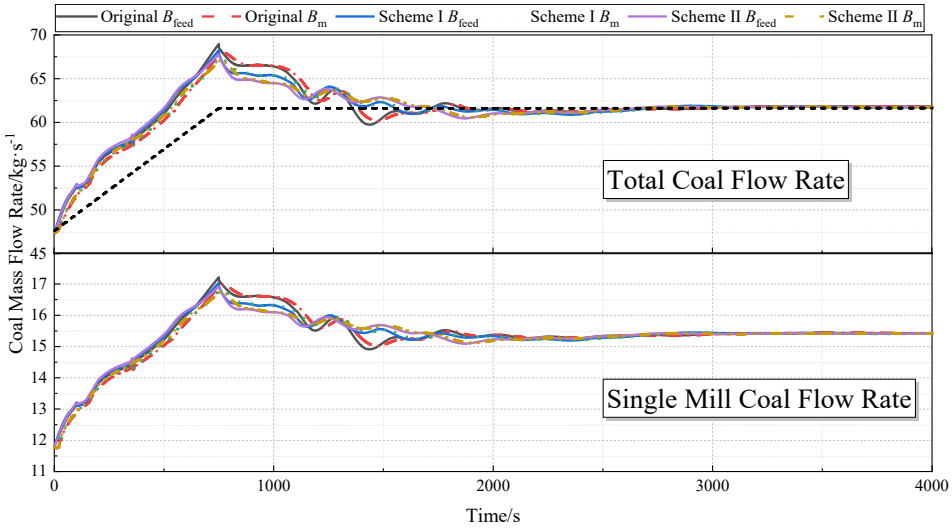

(a)

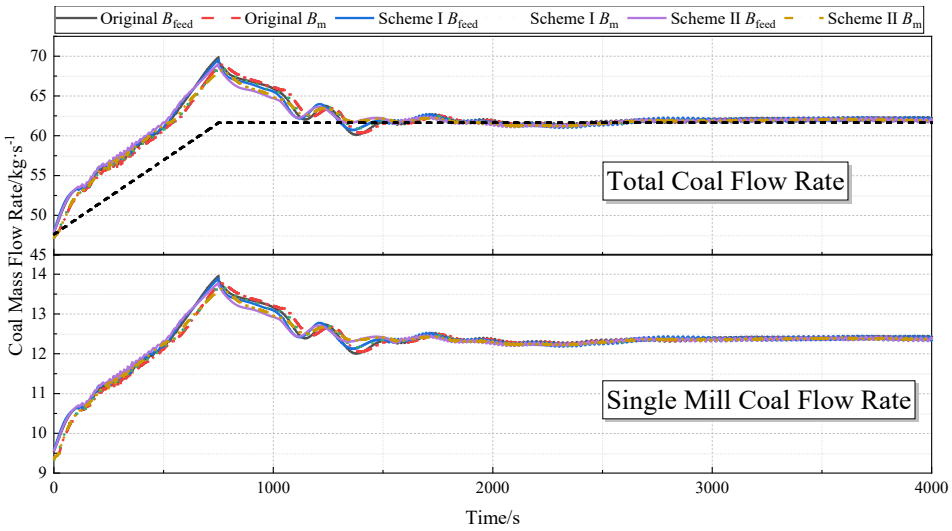

(b)

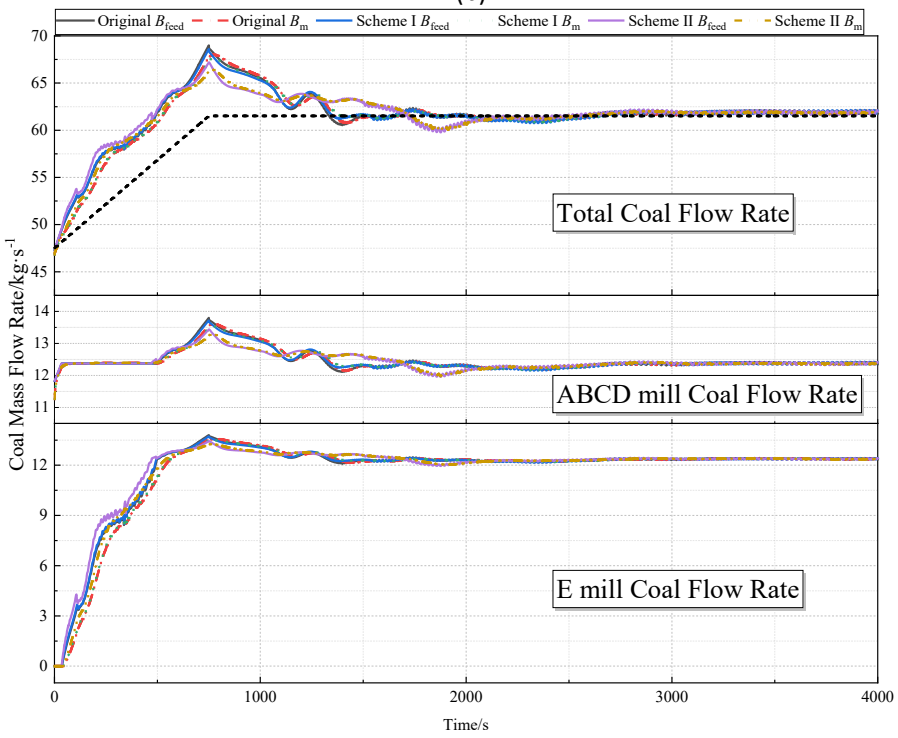

(c)

Fig. 8. Real-time coal consumption during transient processes with V_e=2.0% Pe min^{-1}. (a) four mills in operation; (b) five mills in operation; and (c) four to five mills in operation.

4.2 Energy efficiency analysis of the revised control strategy during load ramping-up transient processes

The absolute output deviation (ΔB) was evaluated for V_e, ranging from 1.0% to 2.5% Pe min^{-1} across the three operational modes, comparing the original and revised strategies during the load cycling. As shown in Fig. 9, ΔB increased with the increase in V_e notably under the same pulverizing system operating mode, indicating that the faster the load change rate, the greater the pulverized coal output fluctuation relative to the pulverizing system's coal feed rate. With the implementation of the optimized control strategy, ΔB decreased to varying degrees across different V_e. Notably, when four mills were in operation with V_e equaling 2.5% Pe min^{-1}, ΔB experienced the most significant reduction, decreasing by as much as 216 kg. When V_e equals 1.0% Pe min^{-1}, the decrease in ΔB was not significant, and in some cases, it may even increase. This indicates that under lower V_e, the original control strategy is already sufficient to meet the output response requirements, and introducing the

optimized control strategy in such scenarios may actually backfire. In summary, this optimized strategy could enhance the responsiveness of the pulverizing system's output during the load ramp-up process.

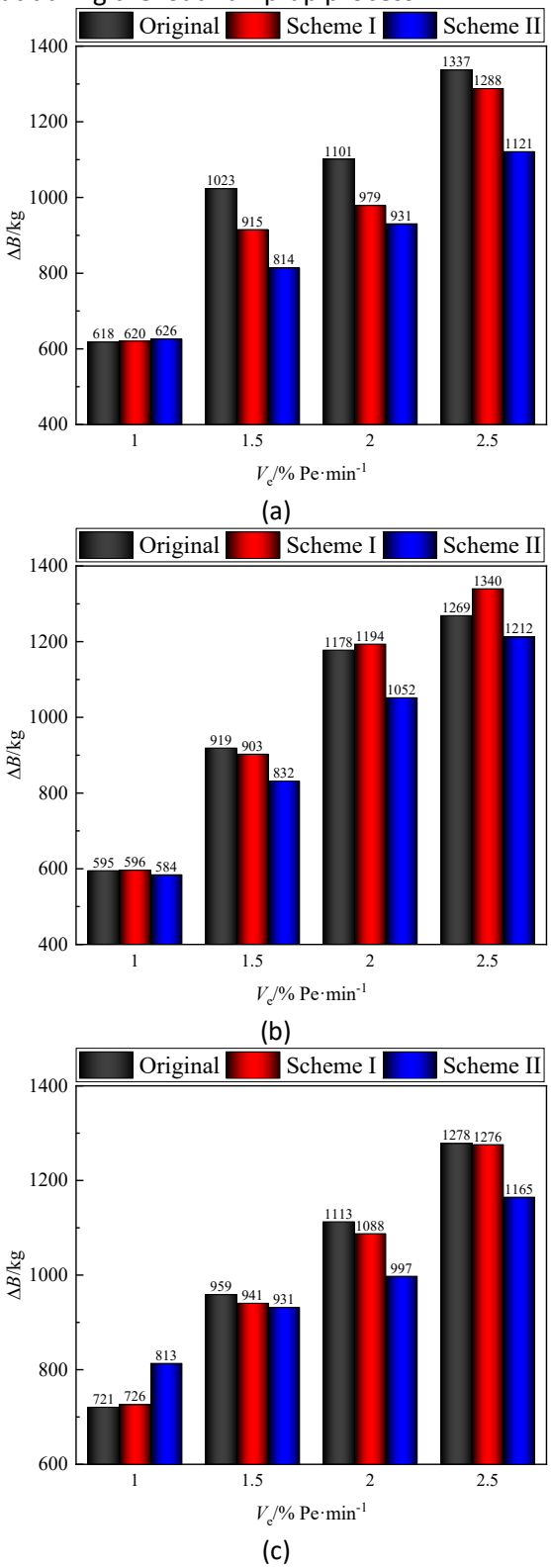

Fig. 9. Comparison of the absolute output deviation with different V_e. (a) four mills in operation; (b) five mills in operation; (c) four to five mills in operation.

5. CONCLUSIONS

This study proposed a comprehensive dynamic model of the pulverizing system and a revised fuel control strategy to align the pulverizing system with the boiler demand and optimize the fuel demand. The study focuses on improving the energy efficiency of thermal power plants. The main conclusions can be drawn from this study as follows:

(1) The MPS pulverizer's comprehensive dynamic simulation model has been developed and validated. A revised control strategy for the fuel demand was proposed based on the concept of main-auxiliary coordinated and synchronized regulation of coal-fired power units.

(2) The optimized fuel control strategy allows the real-time pulverized coal output of the pulverizing system to more closely match the fuel requirements of a boiler during load cycling processes.

(3) The absolute pulverized coal output deviation was reduced by up to 216 kg with four mills, 126 kg with five mills, and 116 kg during the transition from four to five mills. When four coal mills were in operation, the reduction accounted for 0.09% of the pulverizing system's output during the load change process, which totaled 246.02 t.

ACKNOWLEDGEMENT

This work was supported by the Natural Science Basic Research Plan in Shaanxi Province of China (Program No. 2021JLM-34).

REFERENCE

[1] China Electricity Council. (2024, July 10). T*he China Electricity Council released the "Annual Development Report of China's Power Industry 2024."* https://cec.org.cn/detail/index.html?3-334911.

[2] Wang CY, Song JW. Performance assessment of the novel coal-fired combined heat and power plant integrating with flexibility renovations. Energy 2023;263.

[3] Liu M, Ma GF, Wang S, Wang Y, Yan JJ. Thermo-economic comparison of heat–power decoupling technologies for combined heat and power plants when participating in a power-balancing service in an energy hub. Renewable and Sustainable Energy Reviews 2021; 152:111715.

[4] Blanquiceth J, Cardemil JM, Henríquez M, Escobar R. Thermodynamic evaluation of a pumped thermal electricity storage system integrated with largescale thermal power plants. Renew Sustain Energy Rev 2023; 175:113134.

[5] Agrawal A, Panigrahi BK, Subbarao PMV. Review of control and fault diagnosis methods applied to coal mills. Journal of Process Control 2015; 32:138-153.
[6] Gao YK, Zeng DL, Liu JZ. Modeling of a medium speed coal mill. Powder Technology 2017; 318:214-223.
[7] Łabęda-Grudziak, Zofia M. The Disturbance Detection in the Outlet Temperature of a Coal Dust–Air Mixture on the Basis of the Statistical Model. Energies 2022; 15:7302.
[8] Hu Y, Ping BY, Zeng DL, Niu YG, Gao YK. Modeling of coal mill system used for fault simulation. Energies 2020 13:1784.
[9] Huang CZ, Qu SY, Ke ZW, Zheng W. Dual fault warning method for coal mill based on Autoformer WaveBound. Reliability Engineering & System Safety 2024; 245:110030.
[10] Wang YL, Ma ZY, Shen YL, Tang YJ, Ni MJ, Chi Y, et al. A power-saving control strategy for reducing the total pressure applied by the primary air fan of a coal-fired power plant. Applied energy 2016; 175:380-388.
[11] Liang XF, Li YG, Wu X, Shen J. Nonlinear modeling and inferential multi-model predictive control of a pulverizing system in a coal-fired power plant based on moving horizon estimation. Energies 2018; 11:589.
[12] Gao YK, Zeng DL, Liu JZ, Jian YF. Optimization control of a pulverizing system on the basis of the estimation of the outlet coal powder flow of a coal mill. Control Engineering Practice 2017; 63:69-80.
[13] Wang CY, Liu M, Li BX, Liu YW, Yan JJ. Thermodynamic analysis on the transient cycling of coal-fired power plants: simulation study of a 660 MW supercritical unit. Energy 2017; 122:505–527.
[14] Liu ZF, Wang CY, Fan JL, Liu M, Xing Y, Yan JJ. Enhancing the flexibility and stability of coal-fired power plants by optimizing control schemes of throttling high-pressure extraction steam. Energy 2024; 288:129756.
[15] Wang CY, Qiao YQ, Liu M, Zhao YL Yan JJ. Peak shaving operational optimization of supercritical coal-fired power plants by revising control strategy for water-fuel ratio. Applied Energy 2018; 216:212-223.